



---

**Static mode study of the incidence angle and wavelength effects on series resistance of a parallel vertical junction silicon solar cell under monochromatic illumination and under irradiation**

**Alioune Badara Dieng<sup>1</sup>, Fakoro Souleymane Dia<sup>2</sup>, Senghane Mbodji<sup>3</sup>, Birame Dieng<sup>3</sup>**

<sup>1</sup>Faculty of Science and Technology, University Cheickh Anta Diop, Dakar, Senegal

<sup>2</sup>Faculty of Science and Technology, University Cheickh Anta Diop, Dakar, Senegal

<sup>3</sup>Physics Department, Alioune Diop University, Bambey, Senegal Physics Department, Alioune Diop University, Bambey, Senegal

---

**Abstract** In this article, we made atheoretical study of a parallel vertical junction solar cell under monochromatic illumination, in static mode and under irradiation.

The resolution of the continuity equation that governs the generation, the recombinations and the process of diffusion of the electrons in the base allowed us to establish the expression of the electrons density in the base and to deduce expressions of the photocurrent density and phototension depending on the wavelength  $\lambda$ , the recombination velocity at the junction  $S_f$ , the incidence angle of the solar radiation and the irradiation parameters.

The expression of the series resistance has been established from those of phototension and photocurrent density.

We studied the influence of wavelength and incidence angle variations on the minority carriers density in the base, the photocurrent density, the phototension and finally on the series resistance.

---

**Keywords** silicon solar cell, vertical junction, wavelength, incidence angle, irradiation, Series resistance

---

**1. Introduction**

We will perform, through this paper a theoretical study of a parallel vertical junction solar cell under monochromatic illumination, in static mode and under irradiation.

The resolution of the continuity equation will enable us to establish the expression of the minority density charge carriers in the base and deduce those of the photocurrent density and the phototension.

The expression of the Shunt resistance will be subsequently obtained.

We will study, in this article, the impact of the change in wavelength and the incidence angle on the density of the minority carriers in the base, the photocurrent density, the phototension and finally on the series resistance.

**2. Theory**

We consider a  $n^+ - p - p$  parallel vertical junction solar cell whose structure can be represented as follows:



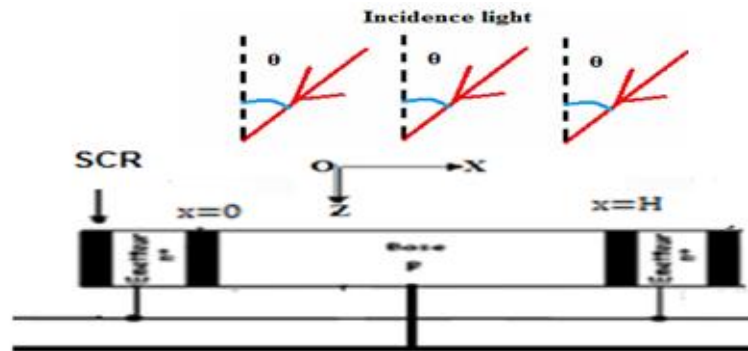


Fig 1: parallel vertical junctions of a solar cell

When the solar cell is illuminated, there is a creation of electron-hole pairs in the base.

The behaviour of the minority carriers in the base (the electrons) is governed by the continuity equation which integrates all the phenomena causing the variation of the density of the electrons according to the width  $x$  of the base, its depth  $z$ , the recombination velocity at the junction, of the wavelength, incidence angle and irradiation parameters.

The resolution of this equation will enable us afterwards to express on the one hand the density minority charge carriers from the base and deduce those of the quantities and other solar cell electrical parameters.

The continuity equation in static mode is presented in the form below:

$$D \cdot \frac{\partial^2 \delta(x)}{\partial x^2} - \frac{\delta(x)}{\tau} = -G(z, \lambda, \theta) \quad (1)$$

$\delta(x)$  describes the density of minority carriers in photo-generated charge.

$D$  is the coefficient diffusion.  $\tau$  is the average lifetime of carriers.

$G(z, \lambda, \theta)$  is the overall generation rate of the minority charge carriers according to the depth  $z$  of the base, the wavelength and incidence angle.

The continuity equation can be written again as follows:

$$\frac{\partial^2 \delta(x)}{\partial x^2} - \frac{\delta(x)}{L^2} + \frac{G(z, \lambda)}{D} = 0 \quad (2)$$

$L(kl, \phi) = \frac{1}{\sqrt{kl\phi + \frac{1}{L_0^2}}}$  is the diffusion length [1].  $L_0$  is the diffusion length with the absence of irradiation;

$kl$  and  $\phi$  indicate the coefficient of damage and the irradiation energy.

The expression of the overall generation of minority charge carriers' rate is of the form: [2]

$$G(z, \lambda, \theta) = \alpha(\lambda)(1 - R(\lambda)) \cdot F \cdot \exp(-\alpha_i \cdot z) \cdot \cos(\theta) \quad (3)$$

$R(\lambda)$  is the monochromatic reflection coefficient;  $F$  is the flux of incident photons resulting from a monochromatic radiation.  $\alpha$  is the coefficient of monochromatic absorption and  $\theta$  the incidence angle.

$$\frac{\partial^2 \delta(x)}{\partial x^2} - \frac{\delta(x)}{L^2} = -\frac{G(z, \lambda)}{D} \quad (4)$$

## 2.1. Solution of the continuity equation

- Special solution:

$$\delta_1(x) = \frac{L^2}{D} \alpha(\lambda)(1 - R(\lambda)) \cdot F \cdot \exp(-\alpha_i \cdot z) \cdot \cos(\theta) \quad (5)$$



-solution of the second member equation:

$$\delta_2(x) = A \cosh\left(\frac{x}{L}\right) + B \sinh\left(\frac{x}{L}\right) \quad (6)$$

-thus the general solution is:

$$\delta(x, z, \lambda, Sf, kl, \phi, \theta) = \left[ A \cosh\left(\frac{x}{L(kl, \phi)}\right) + B \sinh\left(\frac{x}{L(kl, \phi)}\right) + \frac{L^2(kl, \phi)}{D} \cdot \alpha(\lambda)(1 - R(\lambda)) \cdot F \cdot \exp(-\alpha, z) \cdot \cos(\theta) \right] \quad (7)$$

2.2. Find the coefficients A and B:

- The boundary conditions:

-Therefore, in the junction ( $x = 0$ ) we have:

$$D \cdot \left. \frac{\partial \delta(x, z, \lambda, kl, \phi, \theta)}{\partial x} \right|_{x=0} = Sf \cdot \delta(x, z, \lambda, kl, \phi, \theta) \Big|_{x=0} \quad (8)$$

$Sf$  is the recombination velocity at the junction. This is a phenomenological parameter that describes how the base minority carriers go through the junction. It can be divided into two terms [3].

$$\text{We have } Sf = Sf_o + Sf_j$$

$Sf_o$  induced by the shunt resistance, is the intrinsic recombination velocity. It depends only on the intrinsic parameters of the solar cell.

$Sf_j$  reflects the current which is imposed by an external charge and thus defining the operating point of the solar cell

-At The middle of the base ( $x = \frac{H}{2}$ ). The structure of the solar cell, with two similar junctions on either side of the base, portends the equation (9) below:

$$D \cdot \left. \frac{\partial \delta(x, z, kl, \lambda, \phi, \theta)}{\partial x} \right|_{x=H/2} = 0 \quad (9)$$

H is the thickness of the solar cell's base

### 3. Results and Discussion

#### 3.1. Density profile minority charge carriers in the base:

Figure 2 below shows the profile of the electron density in the base according to the wavelength for different values of the incidence angle.

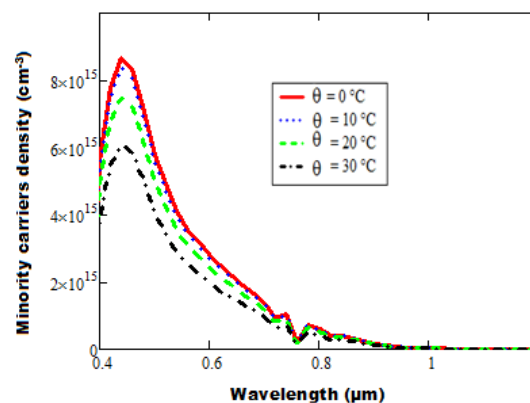


Figure 2: Variation of the minority carriers density according to the wavelength for different values of the incidence angle.

$$H=0,03\text{cm}, Z=0,0001\text{cm}, L_o=0,01\text{cm}, kl=10\text{ cm}^2/\text{s}, \phi=50\text{Mev}, Sf=10\text{ cm/s}$$



The analysis of the curves shows that the minority carriers charges density in the base increases according to the wavelength in the interval  $[0.40 \mu\text{m}; 0.50\mu\text{m}]$  and progressively decreases in the rest of the visible spectrum by undergoing slight fluctuations around  $\lambda = 0.8 \mu\text{m}$ .

The minority carrier charges density in the base decreases when the incidence angle of solar radiation increases.

The majority of photons emitted by the sun are in the visible domain and the charge carriers density depends on the photon flux of the solar radiation, which increases according to the wavelength up to the peak  $\lambda = 0.5 \mu\text{m}$  and then decreases progressively with small variations noted towards the end of the visible spectrum.

In the interval  $[0.40 \mu\text{m}; 0.50 \mu\text{m}]$ , the generation of carriers is very high with sufficiently energetic photons absorbed near the illuminated surface and the surface recombinations are weak.

The decrease of the minority carrier density result from that of the photons flux which are less and less energetic.

The photogenic carriers have less and less energy and the volume recombinations combined to that surface reduce the density.

Indeed low energy photons are absorbed in volume and it must also take into account the phenomena of luminous waves attenuation.

For a flat solar cell, the amount of photons absorbed depends on the incidence angle of solar radiation. The more the incidence angle increases, fewer energy is absorbed, which decreases the charge carriers generation.

### 3.2. Photocurrent density profile

The expression of the photocurrent density of the solar cell is obtained from the gradient of the minority carriers density in the base according to Fick's law. We have:

$$J_{ph} = 2q \cdot D \cdot \left. \frac{\partial \delta(x, z, S_f, \lambda, kl, \phi, \theta)}{\partial x} \right|_{x=0} \quad (10)$$

Where  $q$  is the elementary charge of electricity. From where:

$$J_{ph} = 2q \frac{S_f L^3 \cdot \alpha(\lambda)(1 - R(\lambda)) \cdot F \cdot \exp(-\alpha_r \cdot z) \cos(\theta) \cdot \tanh\left(\frac{H}{2L}\right)}{S_f \cdot L + D \tanh\left(\frac{H}{2L}\right)} \quad (11)$$

Figure 3 below shows the profile of the photocurrent density according to the wavelength for different values of the incidence angle.

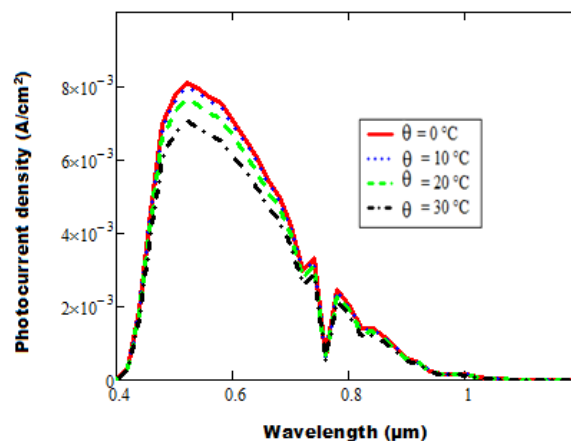


Figure 3: Variation of the photocurrent density according to the wavelength for different values of the incidence angle.

$$H=0,03\text{cm}, Z=0,0001\text{cm}, L_0=0,01\text{cm}, kl=10\text{cm}^2/\text{s}, \phi=50\text{Mev}, S_f=10\text{cm}/\text{s}$$



The analysis of the curves shows that the photocurrent density variations according to the wavelength for different incidence angle values of the solar radiation are similar to those of the minority charge carriers density of the base.

The contribution of the minority charge carriers from the base in the current delivered by the solar cell is related to the variations of the density of these carriers according to Fick's law.

**3.3. Phototension profile**

The phototension created by accumulation of charge carriers at the junction is obtained from Boltzmann's relationship:

$$V = V_T \cdot \ln \left[ 1 + \frac{N_b}{n_0^2} \cdot \delta(0, z, \lambda, kl, \phi, Sf, \theta) \right] \tag{12}$$

$V_T = \frac{KT}{e}$  is the thermal tension

Nb: doping rate of acceptor atoms in the base

n0: intrinsic density of carriers at thermal equilibrium. From where:

$$V_{ph} = \frac{KT}{q} \ln \left\{ 1 + \frac{N_b}{n_0^2} \left[ \frac{D \tanh(\frac{H}{2L})}{S_f L + D \tanh(\frac{H}{2L})} \right] \cdot \frac{L^2}{D} \cdot \alpha(\lambda)(1 - R(\lambda)) \cdot F \cdot \exp(-\alpha_i \cdot z) \cdot \cos(\theta) \right\}$$

Figure 4 below shows the profile of the phototension according to the wavelength for different values of the incidence angle.

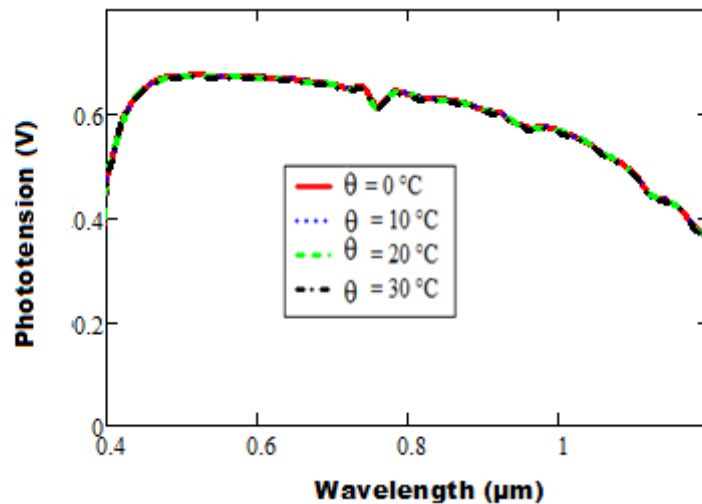


Figure 4: Variation of the phototension according to the wavelength for different values of the incidence angle.

$H=0,03cm, Z=0,0001cm, L_o=0,01cm, kl = 10 cm^2/s, \phi=50Mev, Sf = 10 cm/s$

The variations of the phototension according to the wavelength for different values of the incidence angle follow the same trends as those of the minority carrier density in the base.

The quantity of charges stored on both sides of the junction depends on the photons wavelength, but also on the incidence angle.

**3.4. Current-voltage characteristic:**

Figure 5 below shows the profile of photocurrent density according to the phototension.

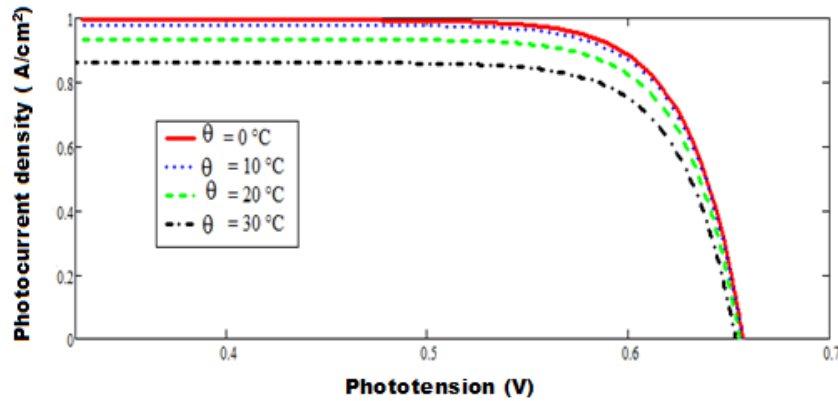


Figure 5: I-V characteristic of the solar cell

The characteristic analysis shows that the phototension is not independent of the photocurrent. The solar cell operates as a real voltage generator in the vicinity of the open circuit and as a real current generator in the vicinity of the short circuit. For each mode of operation, an electrical circuit equivalent to the solar cell is proposed.

**3.5. Series resistance**

Below is the electric model which is equivalent to the solar cell and operating as a real voltage generator:

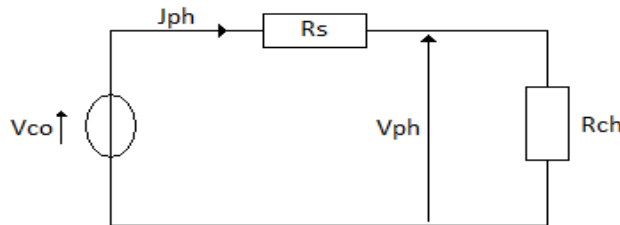


Figure 6: Equivalent circuit of the solar cell (real voltage generator)

From the study of this electrical circuit, the expression of the series resistance is deduced:

$$R_s(S_f, \lambda, kl, \phi, z, \theta) = \frac{V_{CO}(\lambda, kl, \phi, z, \theta) - V_{PH}(S_f, \lambda, kl, \phi, z, \theta)}{J_{PH}(S_f, \lambda, kl, \phi, z, \theta)}$$

Figures 7a and 7b below represent the profile of the series resistance according to the incidence angle for different values of the wavelength.

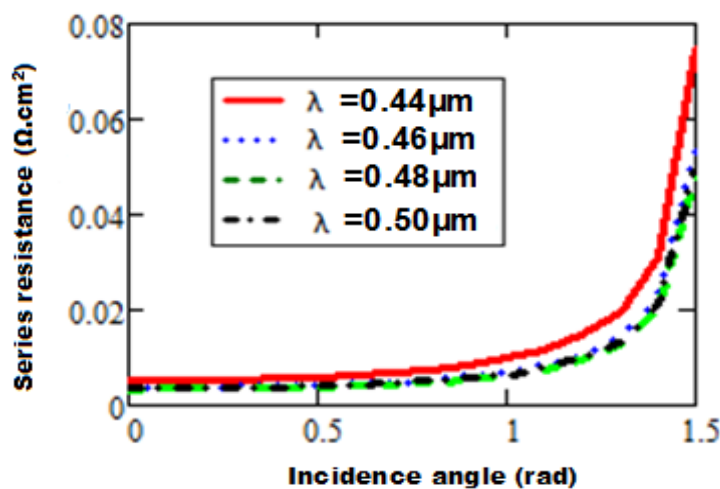


Figure 7a: Variation of the series resistance according to the incidence angle for different values of the wavelength.

$$H=0,03\text{cm}, Z=0,0001\text{cm}, L_0=0,01\text{cm}, kl=10\text{ cm}^2/\text{s}, \phi=50\text{Mev}, S_f=10\text{ cm/s}$$

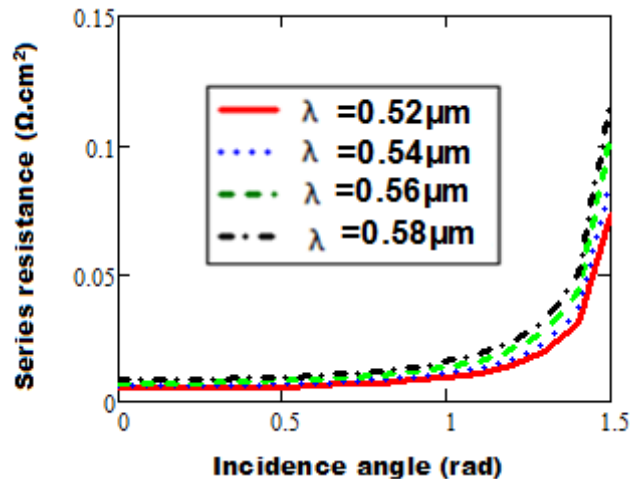


Figure 7b: Variation of the series resistance according to the incidence angle for different values of the wavelength.

$$H=0,03\text{cm}, Z=0,0001\text{cm}, L_o=0,01\text{cm}, kl=10\text{cm}^2/\text{s}, \phi=50\text{MeV}, Sf=10\text{cm/s}$$

The series resistance characterizes the resistive effects of the material and the contact device used.

The analysis of the curves shows that the series resistance increases according to the wavelength in the interval  $[0.40\ \mu\text{m}; 0.50\ \mu\text{m}]$ , then decreases in the rest of the visible spectrum.

When the wavelength increases, the photocurrent density increases in the interval  $[0.40\ \mu\text{m}; 0.50\ \mu\text{m}]$ , which means that the resistive effects of the material reduce so the series resistance.

In the rest of the visible spectrum, we find contrary effects.

The series resistance increases with the incidence angle because the photocurrent density decreases.

#### 4. Conclusion

The resolution of the continuity equation allowed us to obtain the expression of the electrons density in the base and we deduced those of the photocurrent density and the phototension.

From the electric model equivalent to the solar cell when operating in the vicinity of the open circuit, we have established the expression of the series resistance.

We studied, in this paper, the impacts of wavelength and incidence angle variations on the minority carriers density in the base, the photocurrent density, the phototension and finally on the series resistance.

The increase of the wavelength in the interval  $[0.40\ \mu\text{m}; 0.50\ \mu\text{m}]$  resulted in those of minority carrier density in the base, photocurrent density, phototension and a decrease of the series resistance.

In the rest of the visible spectrum, we noted opposite effects.

Indeed, in the interval  $[0.40\ \mu\text{m}; 0.50\ \mu\text{m}]$ , the generation of carriers in the base is very high with a flux of photons in growth and very energetic, the recombinations there are lesser which explains the results.

In the rest of the visible spectrum, the photons are less and less energetic and their flux decreases. The generation rate of the charge carriers decreases as well as the density of these carriers due to the increase of the recombination rate.

The study showed that, the increase of the incidence angle produce a decrease of the minority carrier density in the base, the photocurrent density, the phototension and increase the series resistance.

The increase of the incidence angle cause a decrease of the illuminated area, which affects the photon absorption rate and charge carrier generation.

#### References

- [1]. Th. Flohr and R. Helbig. (1989). Determination of minority-carrier lifetime and surface recombination velocity by optical beam induced current measurements at different light wavelengths, *J. Appl. Phys.*, 66(7), 3060-3065.



- [2]. Kraner. H.W. (1983). Radiation damage in silicon detectors, 2<sup>nd</sup> Pisa meeting on Advanced Detectors, Grosseto, Italy, June 3-7.
- [3]. Mbodji. S., I. Ly, H.L. Diallo, M.M. Dione, O. Diasse and G. Sissoko. (2012). Modeling study of n+/p solar cell resistances from single I-V characteristic curve considering the junction recombination velocity (Sf). Res. J. Appl. Sci. Eng. Techn., 4(1), pp. 1-7.
- [4]. Mathieu H., Fanet. H. (2009). Physique des semiconducteurs et des composants électroniques, 6<sup>th</sup> Ed., Dunod.
- [5]. Green M.A., Emery K., Hishikawa Y., Warta W. (2010). Progress in photovoltaics. Research and applications, Vol. 18, 144–150.
- [6]. Green M.A. (2008). Solar energy. Material and Solar Cells. Vol. 92, 1305–1310.
- [7]. Hu C.C. (2010). Modern semiconductor devices for integrated circuits, Pearson/prentice Hall, New Jersey.
- [8]. Boer K.W. (2010). Introduction to space charge effects in semiconductor, Springer-Verlag.
- [9]. Barsoukov E., Macdonald J.R. (2005). Impedance Spectroscopy, Theory, Experiment and Applications, Wiley, New York.
- [10]. Mathieu H., Fanet H. Physique des semiconducteurs et des composants électronique, 6<sup>th</sup> Ed., Dunod.
- [11]. Green M.A., Emery K., Hishikawa Y., Warta W. (2010). Progress in photovoltaics. Research and applications, Vol. 18, 144–150.
- [12]. Green M.A. (2008). Solar energy. Material and Solar Cells, Vol. 92, 1305–1310.

